The effect of ion exchange and co-precipitation methods on the intercalation of 3-(4-methoxyphenyl)propionic acid into layered zinc hydroxide nitrate

Norhayati Hashim, Zuhailimuna Muda, Illyas Md Isa, Noorshida Mohd Ali, Suriani Abu Bakar & Mohd Zobir Hussein

Journal of Porous Materials

ISSN 1380-2224

J Porous Mater
DOI 10.1007/s10934-017-0438-6

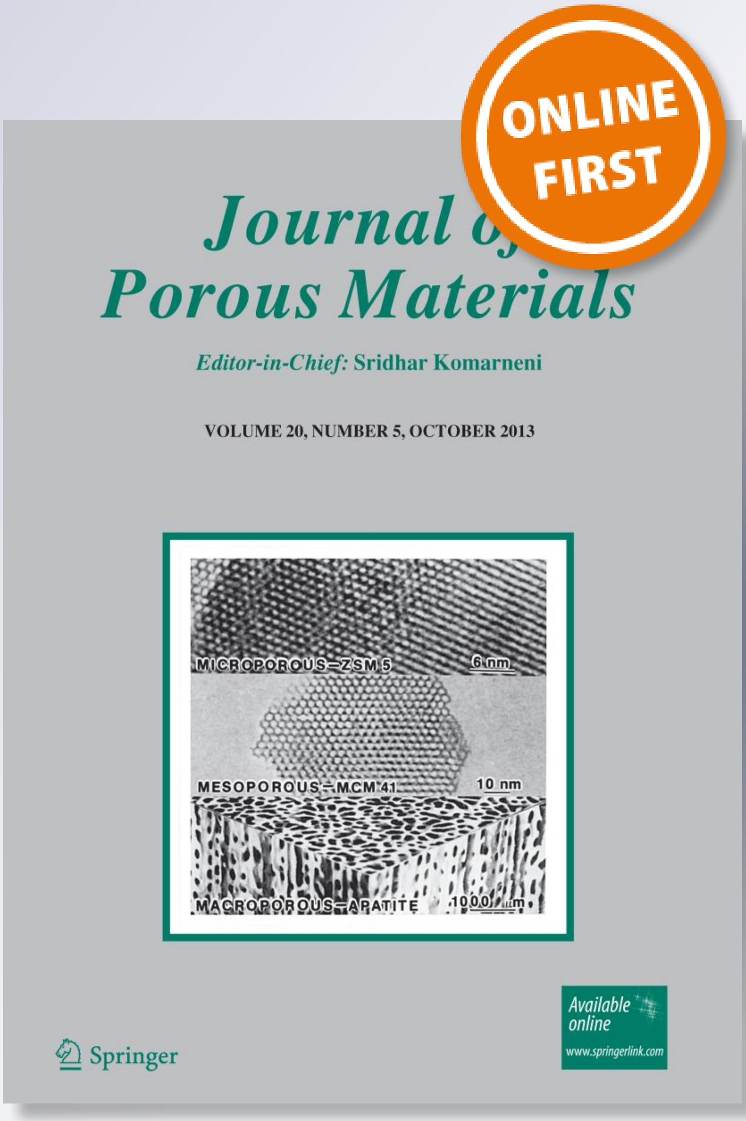

Springer

J Porous Mater
DOI 10.1007/s10934-017-0438-6

The effect of ion exchange and co-precipitation methods on the intercalation of 3-(4-methoxyphenyl)propionic acid into layered zinc hydroxide nitrate

Norhayati Hashim[1,2] · Zuhailimuna Muda[1] · Illyas Md Isa[1,2] · Noorshida Mohd Ali[1,2] · Suriani Abu Bakar[2,3] · Mohd Zobir Hussein[4]

Abstract A new compound, namely zinc hydroxide nitrate-3-(4-methoxyphenyl)propionate (ZHN-MPP) nanocomposite, was prepared using the ion exchange and co-precipitation methods. The resulting nanocomposite was composed of the herbicide MPP sandwiched between ZHN inorganic layers. From PXRD results, the intercalation of MPP anions into the interlayer of ZHN was successful, leading to the expansion of the interlayer of ZHN at 26.9 and 26.1 Å with the ion exchange and co-precipitation methods respectively. The intercalation of layered material is confirmed by PXRD pattern. FTIR spectra for both nanocomposites revealed the presence of MPP in the interlayer of ZHN-MPP nanocomposites. Based on TGA/DTG analysis, the ZHN-MPP nanocomposite prepared by the ion exchange method was found to have greater thermal stability than the one synthesized by the co-precipitation method. The intercalation was also supported by ICP-OES and CHNO-S analysis, which confirmed the presence of C and Zn in the resultant nanocomposites. The surface analyses of both nanocomposites show mesoporous-type material characteristics. However, the co-precipitation method produced nanocomposite with a higher BET surface area compared to the ion exchange method. Overall, the intercalation process decreased the pore size of the nanocomposite compared to the pristine ZHN. The ion exchange method was proven to produce nanocomposite with higher crystallinity and higher thermal stability, whereas the co-precipitation method was proven to produce nanocomposite with a higher surface area compared to the ion exchange method. This work shows that the nanocomposite ZHN-MPP can be synthesized using the ion exchange and co-precipitation methods for the formation of a new generation of agrochemicals.

Keywords Intercalation · Zinc hydroxide nitrate · 3-(4-methoxyphenyl)propionic acid · Ion exchange · Co-precipitation

1 Introduction

Layered materials like layered double hydroxide and layered hydroxide salt are widely applied in the synthesis of novel organic/inorganic nanocomposite materials [1–3]. Various guest anions were intercalated into the interlayer space of layered double hydroxide and layered hydroxide salts due to the positive charge of the hydroxide ions on the brucite-like hydroxide layer [4]. After all, these layered materials are hydrophilic, and it is necessary to intercalate long-chain anionic carbon species between the layers to overcome their hydrophilicity [5]. Their structure, which consists of a positively charged layer, can be expanded or contracted depending on the nature of the interlayer anions [6].

✉ Norhayati Hashim
norhayati.hashim@fsmt.upsi.edu.my

[1] Department of Chemistry, Faculty of Science and Mathematics, Universiti Pendidikan Sultan Idris, 35900 Tanjong Malim, Perak, Malaysia

[2] Nanotechnology Research Centre, Faculty of Science and Mathematics, Universiti Pendidikan Sultan Idris, 35900 Tanjong Malim, Perak, Malaysia

[3] Department of Physics, Faculty of Science and Mathematics, Universiti Pendidikan Sultan Idris, 35900 Tanjong Malim, Perak, Malaysia

[4] Materials Synthesis and Characterization Laboratory, Institute of Advanced Technology, Universiti Putra Malaysia, 43400 Serdang, Selangor, Malaysia

Zinc hydroxide nitrate (ZHN) is an anionic layered material whose composition is $Zn_5(OH)_8(NO_3)_2{\cdot}2H_2O$ [7–9]. ZHN is formed in the monoclinic lattice [10] and this layer is composed of a layer with octahedral coordinated zinc cations, of which one-quarter are displaced out of the layer, leaving an empty octahedral site and forming cationic centres that are tetrahedrally coordinated up and down to the octahedral sheet [11]. Three vertices of the tetrahedron are occupied by hydroxyls, shared with the octahedral sheet, and the apex is occupied by a water molecule. The nitrate anions, however, are freely present in the interlayer spacing [7]. The layers are charged due to the valence vacancies at the tetrahedral zinc atoms.

Depending on the type of material to be obtained, different methods have been used to synthesize ZHN nanocomposite, such as co-precipitation [11, 12], ion exchange [8, 13], the electron beam irradiation technique [14], the pH control method [15], and urea hydrolysis [9]. Above all, ion exchange is frequently used due to its ease of substitution of initial and incoming anions within the interlayer region [16]. This method is useful when the co-precipitation method is inapplicable, such as when the divalent or trivalent metal cations or the anions involved are unstable in alkaline solution, and when intercalated with a bigger size of anion [17]. The co-precipitation method is well known as the cheapest and simplest method of synthesizing nanocomposite, especially for the preparation of ZHN nanocomposite in which ZHN is not being prepared in advance, as previously reported by Arizaga et al. [10] and Liu et al. [9]. In the previous study, MPP herbicide was intercalated into zinc layered hydroxide [18] and layered double hydroxide [19] via the direct method and ion exchange respectively. However, to the best of our knowledge, there are no reports on the intercalation of MPP into layered ZHN using the ion exchange and co-precipitation methods. In a previous study reported by Yang et al. [20], ZHN intercalation compound exhibited stronger interaction with guest species compared to LDH. The strong interaction leads to a slower release of indole-3-acetic acid from ZHN-based nanocomposite than from LDH-based nanocomposite [20]. Prior study also shows that ZHN was successfully intercalated with aspartic acid with high crystallinity and was thermally stable compared to Zn/Al-LDH. Meanwhile, glycine could be easily intercalated into ZHN compared to the Zn/Al-LDH interlayer [21]. This proves that the ZHN intercalation compound is more prone to functionalization than the LDH one. Therefore an attempt is made to intercalate 3-(4-methoxyphenyl)propionic acid (MPP) herbicide into the zinc hydroxide (ZHN) interlayer using the ion exchange and co-precipitation method.

2 Materials and methods

2.1 Materials

Zinc nitrate hexahydrate, $Zn(NO_3)_2{\cdot}6H_2O$ and sodium hydroxide (1 M) were purchased from Systerm, Malaysia. MPP was purchased from Pure Chemistry Scientific. All chemicals were used without further purification.

2.2 Synthesis of ZHN intercalated with MPP via ion exchange method

Layered ZHN was prepared beforehand using the following procedure, as described elsewhere [11]. In brief, it was synthesized by slow addition of NaOH (1 M) into 0.5 M of $Zn(NO_3)_2{\cdot}6H_2O$ solution under magnetic stirring. The final pH was adjusted to 6.5 ± 0.01 under a nitrogen atmosphere. The product obtained was centrifuged, washed with deionized water, and dried in an oven.

Later, about 0.8 g of ZHN was reacted with 50 ml of MPP solution (0.025, 0.05, and 0.10 M) and magnetically stirred for 2 1/2 h. The slurry was then aged in an oil bath shaker at 70 °C for 24 h before being centrifuged and washed with deionized water. The final product was dried and labelled as ZHN-MPP 1. It was then kept for further characterization and use.

2.3 Synthesis of ZHN intercalated with MPP via co-precipitation method

ZHN-MPP 2 nanocomposite was prepared through the co-precipitation method. The nanocomposite was obtained by a slow addition of MPP solution (0.025, 0.05, and 0.10 M) into the zinc nitrate solution under nitrogen atmosphere. The final pH was adjusted to 7.5 ± 0.01 by the addition of sodium hydroxide (1 M). After that, the same procedure as for the preparation of ZHN-MPP 1 was carried out, where the slurry was aged, washed, and dried. The product labelled as ZHN-MPP 2 was kept in a sample bottle for further characterization and use.

2.4 Characterization

Powder X-ray diffraction (PXRD) patterns were recorded on a Rigaku XRD instrument using CuKα radiation (1.5418 Å) at 30 mA and 40 kV with a scanning speed of 2° min^{-1}. Fourier transform infrared (FTIR) spectra were obtained with a Thermo Nicolet 6700 FTIR spectrometer using a KBr pellet technique in the range of 400–4000 cm^{-1}. Thermal analysis (thermogravimetric and differential thermal analyses, TGA/DTG) of the sample was carried out using a Perkin Elmer Pyris 1 TGA thermo balance with a heating rate of 20 °C min^{-1}. The elemental analysis was carried out by inductively coupled plasma optical emission spectrometry (ICP-OES, model 720 Axial, Agilent) and elemental analyzer (CHNO-S, model Flash EA 1112 Series, Thermo Finnigan) heated with a constant flow of helium stream and enriched with oxygen of 99.9995% purity. Meanwhile, the morphology observations were conducted on a field emission scanning electron microscope (FESEM, model SU 8020 UHR, Hitachi). Surface characterization of the nanocomposites was carried out by the nitrogen gas adsorption–desorption technique at 77 K using a Micromeritics ASAP 2000 and degassed in an evacuated heated chamber at 120 °C overnight.

3 Results and discussion

3.1 Powder X-ray diffraction analysis

Figure 1 show the XRD patterns for ZHN, MPP anions, and the resulting nanocomposite synthesized by the ion exchange method, labelled as ZHN-MPP 1. The XRD pattern of ZHN shows a basal spacing of 9.8 Å at a lower angle of 2θ, due to the intercalation of nitrate ions in the interlayer of the zinc hydroxide layer, which is in agreement with the values reported by Yang et al. [7]. As shown in Fig. 1, the resulting nanocomposite afforded a well-ordered nanolayered structure with expanded basal spacing from 9.8 Å in ZHN to 27.4, 26.9, and 27.1 Å for 0.025, 0.05, and 0.10 M of MPP respectively. The presence of the diffraction peak of the three clear harmonic reflections at the lowest 2θ value is directly related to the basal distance, which clearly confirms the intercalation of the MPP anions into the interlayer gallery of ZHN. Turbostraticity, which is caused by irregular stacking of sequential layers, can also be detected in the ZHN-MPP 1 PXRD pattern by the broadening of basal reflections and the geometry of other diagonal planes at around 30–40 Å, which is similar to what was previously reported by Arizaga et al. [9]. The intensity of the intercalation peak of ZHN-MPP 1 nanocomposite decreases as the concentration of MPP increases from 0.025 to 0.10 M due to the presence of the large amount of MPP in the interlayer, which may interfere with the crystal growth during regeneration [22].

Figure 2 also shows a remarkable increase in the basal spacing of the pristine compounds from 9.8 Å in ZHN to 26.1 Å (0.025 and 0.05 M) and 26.6 Å (0.10 M) in the ZHN-MPP 2 nanocomposite that was successfully synthesized by the co-precipitation method. Similarly to the ion exchange method, the co-precipitation method also afforded the production of highly crystalline and pure phase layered materials. As the concentration of MPP increases to 0.10 M, the XRD pattern shows overlapping peaks, which is due to the presence of unreacted ZHN remaining in the resulting product [23]. The overlapping peaks are clearly observed for the co-precipitation method compared to the ion exchange method, which may be due to the parallel orientation of the nitrate ions, which makes it hard for them to intercalate with the incoming anions [23].

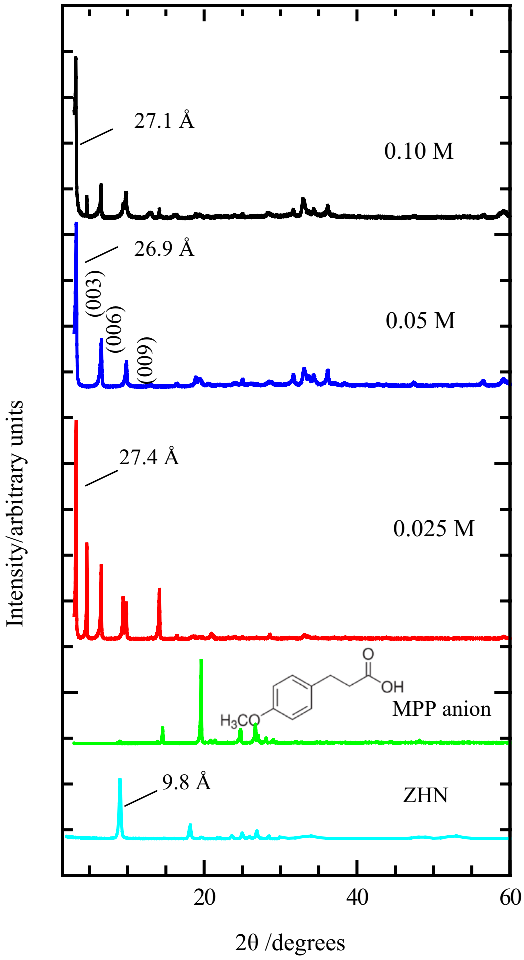

Fig. 1 PXRD patterns for ZHN, MPP anion, and ZHN-MPP 1 nanocomposite with concentrations of 0.025, 0.05 and 0.10 M of MPP

The sharp and intense peak of intercalation of both ZHN-MPP 1 and ZHN-MPP 2 nanocomposites indicates their high crystallinity. A slight difference in basal spacing was detected for both nanocomposites because different planes are refracting due to the layer-charge density or content of water between the layers [24]. Based on the PXRD pattern for both nanocomposites, 0.05-M ZHN-MPP 1 and 0.025-M ZHN-MPP 2 showed three clear harmonic reflection diffractions compared to other concentrations. Therefore, both were chosen for further characterization study.

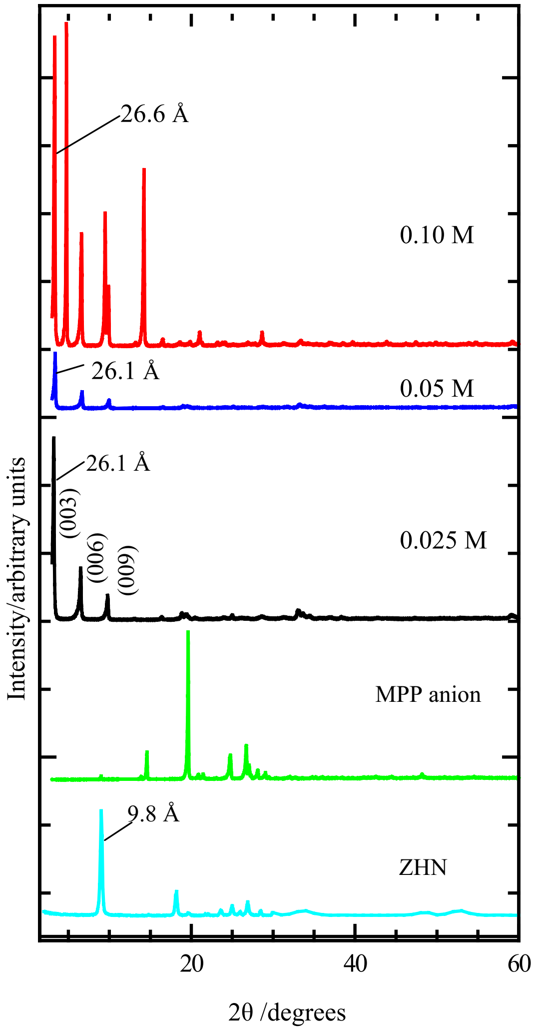

Fig. 2 PXRD patterns for ZHN, MPP anion, and ZHN-MPP 2 nanocomposite with concentrations of 0.025, 0.05 and 0.10 M of MPP

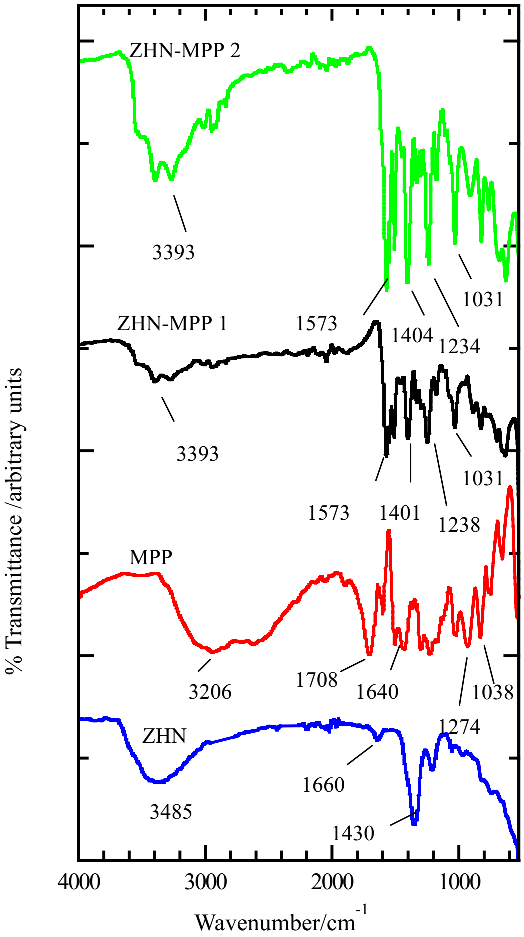

Fig. 3 FTIR spectra of ZHN, MPP, and the ZHN-MPP 1 and ZHN-MPP 2 nanocomposites

3.2 Fourier transform infrared analysis

The FTIR spectra for ZHN, pure 3-(4-methoxyphenyl)propionic acid, and the ZHN-MPP 1 and ZHN-MPP 2 nanocomposites are shown in Fig. 3. The main FTIR absorption bands for ZHN-MPP nanocomposite are listed in Table 1.

For all spectra, broad absorption bands are observed in the range of 3100–3700 cm^{-1} due to the stretching vibrations of the OH group of the lattice and water molecule [7]. The ZHN spectra in Fig. 3 show a typical FTIR spectrum of the host material, ZHN, with nitrate being the counter anion. An absorption band at 1660 cm^{-1} is attributed to the bending mode of water molecules [8]. The most intense absorption band in ZHN is found at 1430 cm^{-1}, which presents a free interlayer nitrate group (symmetry D_{3h}) [9, 25].

FTIR analysis of MPP herbicide showed the spectra of the methoxy group bonding with an aromatic ring displaying an asymmetrical C–O–C stretching band at 1275–1200 cm^{-1}, which was centred at 1274 cm^{-1}, and symmetrical stretching near to 1075–1020 cm^{-1}, which was centred at 1038 cm^{-1}. Meanwhile, the strong and sharp band of C=O for COOH that bonded with the aliphatic alkyl group was centred at 1708 and 1640 cm^{-1} [26].

After the ion exchange reaction for both nanocomposites, the characteristic asymmetric stretching vibration of the nitrate ion at about 1430 cm^{-1} in ZHN disappears and the new peaks at 1401 and 1573 cm^{-1} in the ZHN-MPP 1 spectra and 1404 and 1573 cm^{-1} in the ZHN-MPP 2 spectra appear; they are attributed to the asymmetric and symmetric vibrations of the C=O group. The bands around 1708 and 1640 cm^{-1} (carboxylic group, COOH) in both ZHN-MPP nanocomposite spectra also disappear due to the removal of hydrogen ions from the MPP molecule, which reveals that the species that were intercalated into the ZHN layers were in the anionic form of MPP, otherwise known as 3-(4-methoxyphenyl)propionate [27]. Based on

Table 1 FTIR bands for ZHN-MPP 1 and ZHN-MPP 2 nanocomposites

Characteristic group	MPP	ZHN-MPP 1	ZHN-MPP 2
ν(O–H) in the layer; H_2O	3206	3393	3393
ν_s (C=O) in COOH	1640	–	–
ν_{as}(C=O) in COOH	1708	–	–
$\nu_s(COO^-)$	–	1401	1404
$\nu_{as}(COO^-)$	–	1573	1573
ν_s (C–O–C)	1038	1031	1031
ν_{as} (C–O–C)	1274	1238	1234

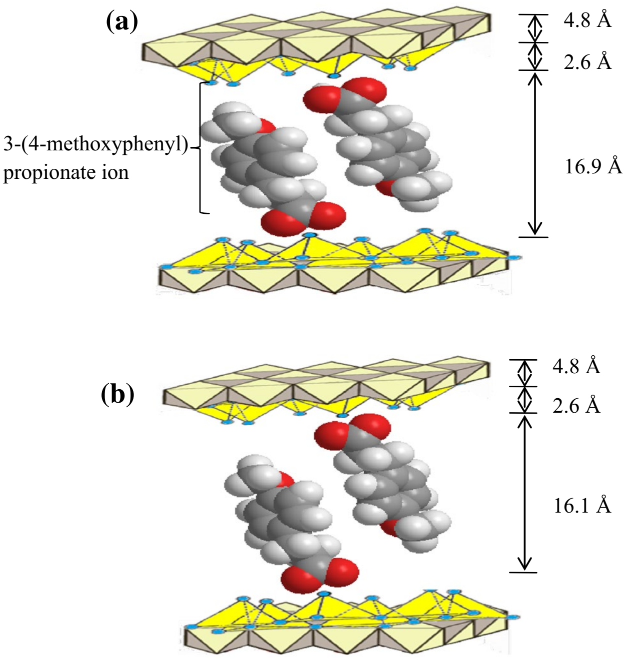

Fig. 4 The proposed orientation of MPP anions intercalated between the ZHN interlayer for the formation of ZHN-MPP 1 **a** and ZHN-MPP 2 **b** nanocomposites estimated by Chemoffice software

the data presented in Table 1, the FTIR spectra of ZHN-MPP 1 show a resemblance to the ZHN-MPP 2 spectra.

3.3 Spatial orientation of MPP between ZHN nanocomposites

The proposed arrangement of the intercalated MPP anions in the interlayer space of ZHN is illustrated in Fig. 4. The proposed spatial arrangement of MPP within the ZHN interlayer region is based on the basal spacing which is obtained from PXRD. The three-dimensional molecular size of MPP was estimated by Chemoffice software. The average basal spacings of the ZHN-MPP 1 and ZHN-MPP 2 nanocomposites were measured as 26.9 and 26.1 Å respectively. Taking into account that the layer thicknesses of ZHN are 4.8 and 2.6 Å for each zinc tetrahedron [28], the expected gallery heights that can be occupied are 16.9 and 16.1 Å for ZHN-MPP 1 and ZHN-MPP 2 respectively. These values are obtained by subtracting the layer thickness plus the height of the Zn^{2+} moiety of the lattice from the basal spacing; that is, 16.9 Å = 26.9 Å − (4.8 + 2.6 + 2.6) Å and 16.1 Å = 26.1 Å − (4.8 + 2.6 + 2.6) Å for ZHN-MPP 1 and ZHN-MPP 2 respectively. MPP anions are vertically aligned in a monolayer stacking order with the carboxylate group pointing toward the ZHN inorganic interlayers. The oxygen atom in the carboxylate groups is directly bonded to the ZHN layers through hydrogen bonding and electrostatic interaction.

3.4 Elemental analysis

The intercalation of MPP anions into the ZHN inorganic interlayer was also confirmed by direct evidence of elemental analysis (CHNS and ICP-OES). Table 2 shows that the percentages of C in ZHN-MPP 1 and ZHN-MPP 2 are 25.40 and 29.55% respectively. Meanwhile, no nitrate has been found in the nanocomposites, which confirms that all nitrate ions have been replaced by MPP anions during the intercalation process. The percentages of Zn were found to be 51.17 and 38.48% for ZHN-MPP 1 and ZHN-MPP 2 respectively. However the percentage loading of MPP anions into the ZHN interlayer gallery is 38.1 and 38.3% for ZHN-MPP 1 and ZHN-MPP 2 respectively. The percentage loading of MPP anions into the ZHN interlayer for both

Table 2 Analyzed chemical composition of ZHN-MPP nanocomposite

Sample	C (%)	N (%)	H (%)	Zn (% w/w)	Anion (% w/w)	Formula
ZHN-MPP 1	25.4	0	3.3	51.2	38.1	$Zn^{2+} (OH)_{0.26} (CH_3OC_6H_4CH_2CH_2COO^-)_{1.74}\cdot 1.04H_2O$
ZHN-MPP 2	29.5	0	4.0	38.4	38.3	$Zn^{2+} (OH)_{0.41} (CH_3OC_6H_4CH_2CH_2COO^-)_{1.59}\cdot 1.50H_2O$

nanocomposite had almost the same value, which possibly indicates that a better interaction took place between the positively charged ZHN layer and the negatively charged MPP anions. However, the high percentage of Zn in ZHN-MPP 1 may be due to the preparation method, as the host is already prepared beforehand and must be rearranged during the ion exchange process [24]. Based on calculation from CHNS, ICP-OES, and TGA/DTG, the formulas of the two nanocomposites were proposed to be Zn^{2+} $(OH)_{0.26}(CH_3OC_6H_4CH_2\ CH_2COO^-)_{1.74}\cdot 1.04\ H_2O$ and Zn^{2+} $(OH)_{0.41}(CH_3OC_6H_4CH_2\ CH_2COO^-)_{1.59}\cdot 1.50\ H_2O$ for ZHN-MPP 1 and ZHN-MPP 2 respectively.

3.5 Thermal analysis

The thermal behaviour of ZHN-MPP nanocomposites was examined using thermogravimetric and differential thermogravimetric analyses (TGA/DTG) (Fig. 5). The thermal analysis curves revealed that a decomposition profile of pure MPP occurred at 258 °C with 98.8% weight loss in one step.

However, ZHN was decomposed in three steps [15]. The first and second steps are simplified as Equations (1) and (2).

$$\text{Step 1: } Zn_5(OH)_8(NO_3)_2 \cdot 2H_2O \rightarrow Zn_5(OH)_8(NO_3)_2 + 2H_2O \quad (1)$$

$$\text{Step 2: } Zn_5(OH)_8(NO_3)_2 \rightarrow 5ZnO + 2NO_2 + 1/2O_2 + 4H_2O \quad (2)$$

In a first step, 3.4% of the weight loss in step 1 at 101 °C was due to the loss of intercalated water [7]. Another 13.4% weight loss at 161 °C in step 2 was due to the decomposition of water formed by dehydroxylation and decomposition

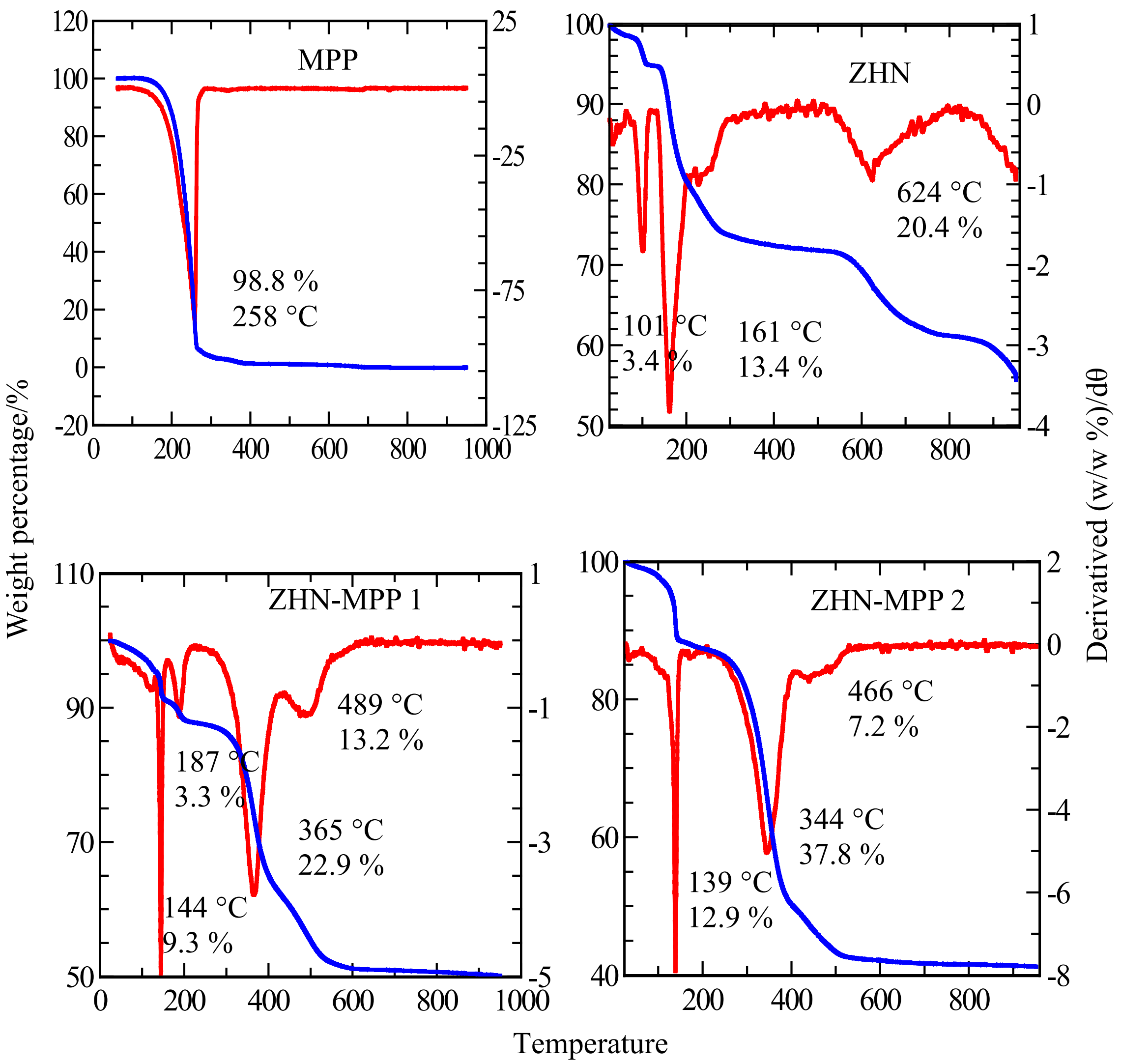

Fig. 5 Thermogravimetric curves of MPP anions, ZHN, and ZHN-MPP 1 and ZHN-MPP 2 nanocomposites

of gas formed from the counterions, NO_2 (Eq. 2). In the previous study, most of the thermal behaviour of ZHN only shows two main peaks [15]. However, in this study another decomposition peak takes place at 624 °C (20.4% weight loss) in the third step, which is probably due to the collapses of the remaining ZHN layered structure and production of zinc oxide phase with wurtzite lattice structure, which is similar to what was reported by Ghotbi et al. [10].

Meanwhile, four main thermal events are clearly observed in the ZHN-MPP 1 nanocomposite. The weight loss in the first stage was 9.3% at 144 °C and was due to the removal of surface physisorbed water molecules [29]. The weight loss of 3.3% at 187 °C was attributed to the removal of interlayer anions and dehydroxylation of the hydroxyl layer [30]. The largest stage of weight loss, occurring at 365 °C (22.9%), was due to the decomposition of the intercalated organic moiety, the MPP anion, between the inorganic ZHN interlayers [31]. At a temperature of 489 °C, 13.2% weight loss occurs, which is due to the collapsing of the layered structure of ZHN [10].

As for the ZHN-MPP 2 nanocomposite, three main thermal stages of weight loss are clearly observed. The first stage of weight loss occurred due to the loss of water of hydration at 139 °C and had a value of 12.9%, which is similar to what was reported in a previous study by Demel et al. [30]. The decomposition of MPP anions takes place in the second stage of weight loss, which occurred at 344 °C and amounted to 37.8%. Similarly to ZHN-MPP 1, the last stage of weight loss of ZHN-MPP 2, which occurred at 466 °C with 7.2% weight loss, was represented by the collapses of the ZHN inorganic interlayer [10].

Generally, the largest percentage of weight loss of ZHN and its nanocomposites occurs in the stage around 150 to 700 °C, leaving the ZnO as a residue. The last stage at around 400 to 700 °C is the slowest stage, due to absorption/adsorption effects on the remaining layered structures and/or the oxides [9]. From the TGA/DTG analysis, both nanocomposites exhibit different thermal behaviours in which ZHN-MPP 1 decomposes in four stages while ZHN-MPP 2 decomposes in three main stages. Besides, ZHN-MPP 1 also shows higher thermal stability than ZHN-MPP 2. The thermal study of both ZHN-MPP 1 and ZHN-MPP nanocomposites revealed that the MPP anions that intercalate in the ZHN interlayer are thermally stable compared to its pure form. This is probably due to a barrier effect, which prevents heat from being transmitted quickly and minimizes

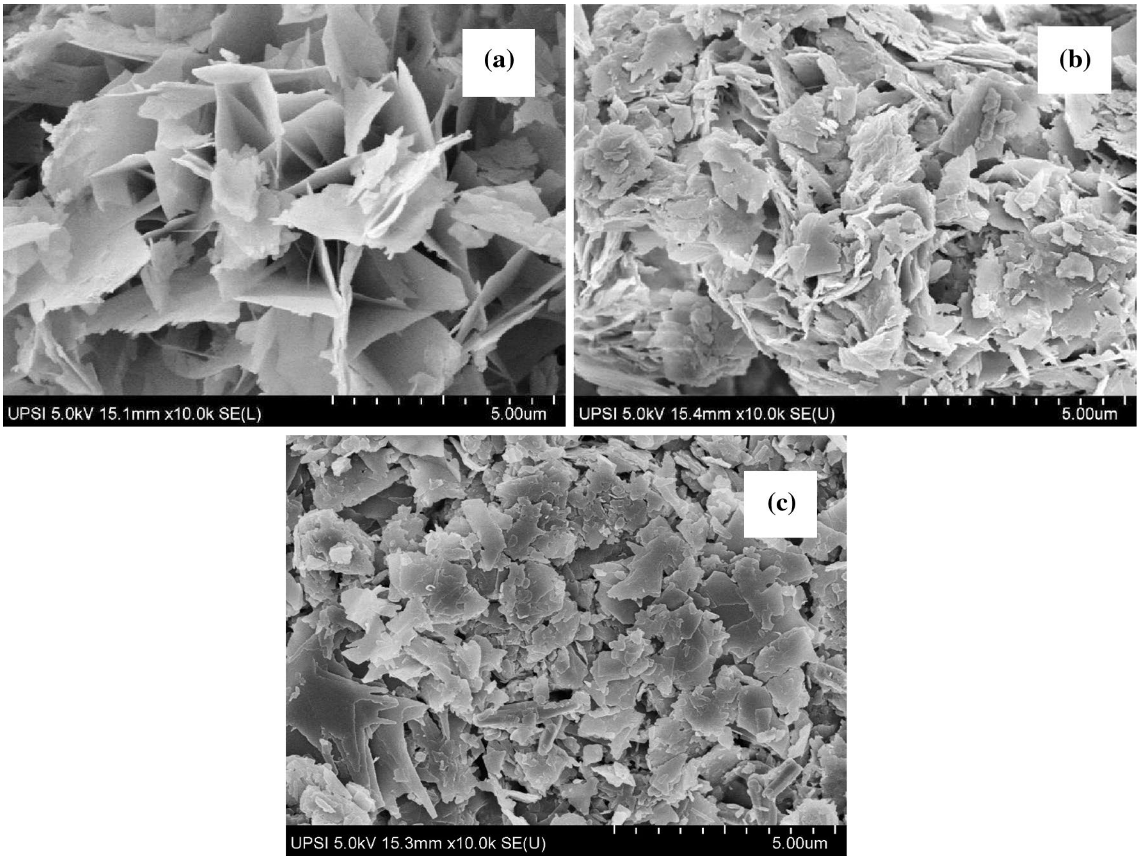

Fig. 6 FESEM image of ZHN **a** and ZHN-MPP 1 **b** and ZHN-MPP 2 nanocomposites with 10k magnification

Table 3 Surface properties of ZHN and ZHN-MPP 1 and ZHN-MPP 2 nanocomposites

Sample	Specific BET surface area (m^2g^{-1})	BJH desorption average pore diameter (nm)
ZHN	47.0	25
ZHN-MPP 1	1.1	22
ZHN-MPP 2	3.3	6

the continuous decomposition of the nanocomposite [32]. Besides, the strong electrostatic interaction between layered ZHN and anionic MPP leads to an increase in thermal stability of the layered structure [9].

3.6 Surface morphology analysis

The surface morphology of layered ZHN and ZHN-MPP 1 and ZHN-MPP 2 nanocomposites at a magnification of ×10k are displayed in Fig. 6. As expected, the ZHN layer possessed a flake-like structure similar to that previously reported by Ghotbi et al. [10] and Hussein et al. [13]. Both ZHN-MPP 1 and ZHN-MPP 2 nanocomposites also show flake-like structures. The intercalation of MPP into the interlayer of layered ZHN has reduced the size of the flakes to a smaller size compared to the morphology of the ZHN layer. After the intercalation, the resulting layered ZHN materials take on new properties that are a function of the intercalant and the way it associates with the host. Therefore both physical and chemical properties including the surface morphology may be affected by the intercalant [25].

3.7 Surface area analysis

The comparison of the surface area and porosity of ZHN and ZHN-MPP nanocomposites intercalated by both methods is shown in Table 3. The intercalation of MPP anions has decreased the BET surface area from 47 m^2g^{-1} for ZHN to 1.1 and 3.3 m^2g^{-1} for ZHN-MPP 1 and ZHN-MPP 2, respectively. Comparing the BET surface areas of nanocomposites prepared by ion exchange and co-precipitation, the latter nanocomposite shows a higher BET surface area. A greater increase of pore surface area is obtained by the co-precipitation method, suggesting that better blending of the MPP into the ZHN occurs by this method compared to

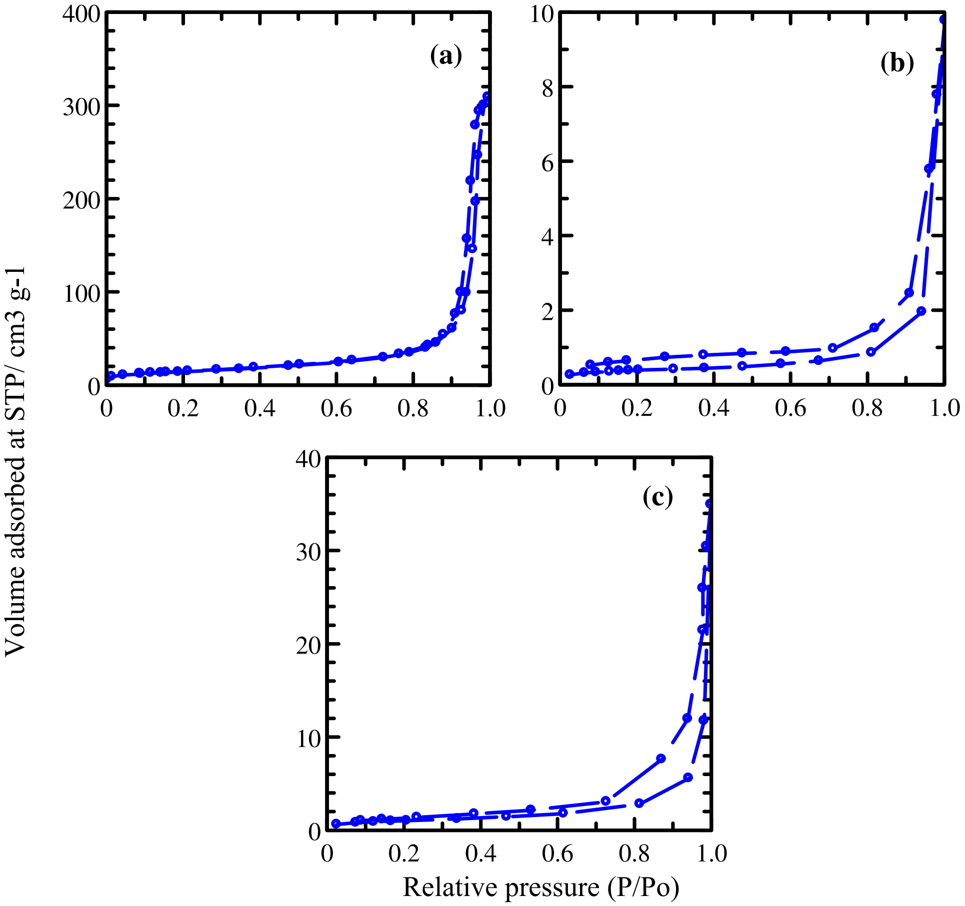

Fig. 7 Adsorption–desorption isotherms of nitrogen gas for ZHN (**a**), ZHN-MPP 1 (**b**), and ZHN-MPP 2 (**c**)

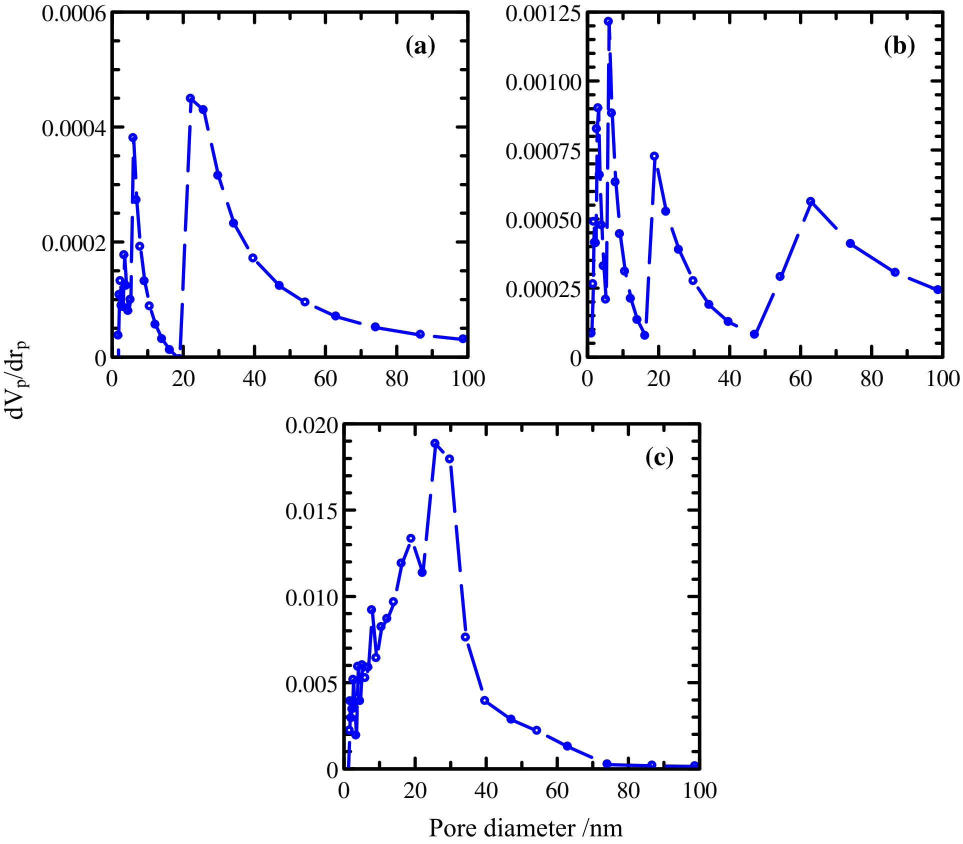

Fig. 8 BJH desorption pore size distributions for ZHN (**a**), ZHN-MPP 1 (**b**), and ZHN-MPP 2 (**c**)

the ion-exchange method, which is in agreement with the previous study by Heraldy et al. [23]. The data also show that the BJH average pore diameter of ZHN decreases from 25 to 22 nm with the ion exchange method and 6 nm with the co-precipitation method. This is due to the closing of the pores by the insertion of MPP into the pores of the ZHN layer [23, 33].

Figure 7 shows the nitrogen-adsorption isotherms for ZHN and for the ZHN-MPP 1 and ZHN-MPP 2 nanocomposites. As shown in the figure, the nitrogen-adsorption isotherms for ZHN and both nanocomposites are type IV isotherms with H3 hysteresis loops based on the International Union of Pure and Applied Chemistry (IUPAC) classification [34], indicating mesoporous-type materials. The adsorption slowly increases at a low relative pressure in the range of 0.0–0.6, which represents the surface monolayer adsorption process. Further increases of the relative pressure (above 0.6) result in rapid adsorption of the adsorbent due to the adsorption of the first multilayer. The presence of the H3 hysteresis loop in layered ZHN and ZHN-MPP 1 and ZHN-MPP 2 nanocomposites reveals that the pores are slit-shaped with nonuniform shape and size. ZHN-MPP 1 showed very much lower maximum adsorption compared to ZHN-MPP 2, due to the high capacity of MPP to intercalate in ZHN-MPP 1 compared to ZHN-MPP 2 nanocomposite.

The BJH pore size distribution for ZHN, ZHN-MPP 1, and ZHN-MPP 2 is shown in Fig. 8. As for ZHN, the pore size distribution is centred at around 25 nm (Fig. 8a). A sharp peak pore size distribution is observed for ZHN-MPP 1 centred at around 6 and 22 nm (Fig. 8b). On the other hand, ZHN-MPP 2 showed a sharp peak with pore size distribution centred at around 6, 18, and 63 nm (Fig. 8c). In general, the pore size distributions do not show the formation of regular mesopores in the layered ZHN-nanocomposites, but could reveal the contribution of irregular mesoporous interparticulate void space [15].

4 Conclusions

ZHN has been successfully intercalated with MPP anions via the ion exchange and co-precipitation methods. The ion exchange method produces a bigger expansion of the interlayer at 26.9 Å compared to the co-precipitation method with the expansion of the interlayer of ZHN at 26.1 Å. Both the ion exchange and the co-precipitation method afforded a well-ordered crystalline structure of the resultant nanocomposites. The interlayer spacing of the nanocomposite synthesized by the ion exchange method is bigger than that of the nanocomposite synthesized by the co-precipitation method. The FTIR spectra for both nanocomposites revealed that nitrate ions were replaced by MPP anions in the interlayer of ZHN. Apparently the intercalation process did affect the surface area and the pore size of the resulting materials. However, both resulting nanocomposites are mesoporous-type of materials. Evaluation of the thermal properties of ZHN-MPP nanocomposites proved that the intercalated MPP had higher thermal stability than its pure form. Whereas, ZHN-MPP 1 was proven to be more thermally stable than ZHN-MPP 2. The ion exchange method was successfully synthesis nanocomposite with higher crystalinity and higher thermal stability. As for co-precipitation method, the resulting nanocomposite has a larger surface area compared to the nanocomposite prepared by co-precipitation method. However the present result confirms that both methods can synthesis ZHN nanocomposite to be an outstanding biocompatible inorganic host for further applications.

Acknowledgements The author is grateful to the support for the research provided by KPM under FRGS Grant No. 2014-0031-101-02. NH thanks UPSI for all funding and support for this research.

Compliance with ethical standards

Conflict of interest The authors declare that they have no conflict of interest.

References

1. A. Yasutake, S. Aisawa, S. Takahashi, H. Hirahara, E. Narita, J. Phys. Chem. Solids **69**, 1542 (2008)
2. Z.B. Jubri, M.Z. Bin Hussein, A.H. Yahaya, Z. Zainal, J. Porous Mater. **19**, 45 (2012)
3. K. Muramatsu, O. Saber, H. Tagaya, J. Porous Mater. **14**, 481 (2007)
4. J.W. Lee, W.C. Choi, J.-D. Kim, CrystEngComm **12**, 3249 (2010)
5. A. Zimmermann, S. Jaerger, S. F. Zawadzki, F. Wypych, J. Polym. Res. **20**, 224 (2013)
6. S.M.N. Mohsin, M.Z. Hussein, S.H. Sarijo, S. Fakurazi, P. Arulselvan, T.-Y.Y. Hin, Chem. Cent. J. **7**, 26 (2013)
7. W. Yang, L. Ma, L. Song, Y. Hu, Mater. Chem. Phys. **141**, 582 (2013)
8. A.C.T. Cursino, J.E.F.D.C. Gardolinski, F. Wypych, J. Colloid Interface Sci. **347**, 49 (2010)
9. G.G.C. Arizaga, K.G. Satyanarayana, F. Wypych, Solid State Ionics **178**, 1143 (2007)
10. M.Y. Ghotbi, N. Bagheri, S.K. Sadrnezhaad, Adv. Powder Technol. **23**, 279 (2012)
11. J. Liu, X. Zhang, Y. Zhang, ACS Appl. Mater. Interfaces **7**, 11180 (2015)
12. G.G.C. Arizaga, J.E.F.D.C. Gardolinski, W.H. Schreiner, F. Wypych, J. Colloid Interface Sci. **330**, 352 (2009)
13. R. Marangoni, L.P. Ramos, F. Wypych, J. Colloid Interface Sci. **330**, 303 (2009)
14. H.S. Bae, H. Jung, Bull. Korean Chem. Soc. **33**, 1949 (2012)
15. M. Z. Bin Hussein, M. Y. Ghotbi, A. H. Yahaya, M. Z. Abd Rahman, Solid State Sci. **11**, 368 (2009)
16. M. Z. Hussein, N. Hashim, A. H. Yahaya, Z. Zainal, J. Exp. Nanosci. **5**, 548 (2010)
17. H.Y. He, Mater. Sci. Semicond. Process. **31**, 200 (2015)
18. N. Hashim, Z. Muda, S.A. Hamid, I. Isa, A. Kamari, A. Mohamed, Z. Hussein, S.A. Ghani, J. Phys. Chem. Sci. **1**, 1 (2014)
19. Z. Muda, N. Hashim, N.H. Yusri, I.M. Isa, A. Kamari, A. Mohamed, N.M. Ali, Nano Hybrids **8**, 39 (2014)
20. J.H. Yang, Y.S. Han, M. Park, T. Park, S.J. Hwang, J.H. Choy, Chem. Mater. **19**, 2679 (2007)
21. G.C.G. Arizaga, J. Solid State Chem. **185**, 150 (2012)
22. F.R. Costa, A. Leuteritz, U. Wagenknecht, M. Auf der Landwehr, D. Jehnichen, L. Haeussler, G. Heinrich, Appl. Clay Sci. **44**, 7 (2009)
23. E. Heraldy, R.W. Suprihatin, Pranoto, Mater. Sci. Eng. **107**, 1 (2016)
24. B. Saifullah, M. Z. Hussein, S. H. Hussein-Al-Ali, P. Arulselvan, S. Fakurazi Drug Des. Dev. Ther. **7**, 1365 (2013)
25. A.F. Abdul Latip, M.Z. Hussein, J. Stanslas, C.C. Wong, R. Adnan, Chem. Cent. J. **7**, 119 (2013)
26. M.Z. Hussein, N. Hashim, A.H. Yahaya, Z. Zainal, Solid State Sci. **12**, 770 (2010)
27. A.M. Bashi, M.Z. Hussein, Z. Zainal, D. Tichit, J. Solid State Chem. **203**, 19 (2013)
28. M.Z. Hussein, N.S.S.A. Rahman, S.H. Sarijo, Z. Zainal, Int. J. Mol. Sci. **13**, 7328 (2012)
29. M. Silion, D. Hritcu, G. Lisa, M.I. Popa, J. Porous Mater. **19**, 267 (2012)
30. J. Demel, P. Kubát, I. Jirka, P. Kovář, M. Pospíšil, K. Lang, J. Phys. Chem. C **114**, 16321 (2010)
31. S.H. Sarijo, S.A.I.S.M. Ghazali, M.Z. Hussein, N.J. Sidek, J. Nanoparticle Res. **15**, 1536 (2013)
32. W. Hu, B. Yu, S.-D. Jiang, L. Song, Y. Hu, B. Wang, J. Hazard. Mater. **300**, 58 (2015)
33. N. Hashim, M. Z. Hussein, A. H. Yahaya, Z. Zainal, Malays. J. Anal. Sci. **11**, 1 (2007)
34. K.S.W. Sing, D.H. Everett, R.A.W. Haul, L. Moscou, R.A. Pierotti, J. Rouquérol, T. Siemieniewska, Pure Appl. Chem. **57**, 603 (1985)